

# Characterization of Optical Data Links for the CMS Experiment

V. Arbet-Engels, G. Cervelli, K Gill, R. Grabit, C. Mommaert, G. Stefanini, and F. Vasey

CERN, CH-1211, Geneva 23, Switzerland.

vincent.arbet.engels@cern.ch

## Abstract

The complex data acquisition system of the CMS tracker will make extensive use of optical fibre links for: (a) the analogue readout of detector signals from the front-end electronics, (b) the digital communication between the front-end and the back-end electronics such as the timing and trigger distribution and the slow control and monitoring of the detector. The analogue and digital links are based on a common architecture with identical edge-emitting lasers at 1310nm, PIN photodiodes, and single mode optical fibres. One channel link demonstrators built with optoelectronic components representative of those to be used in the future readout system have been fully characterized. The analogue link overall performance is discussed in terms of its static and dynamic responses and is shown to meet the technical specifications of the full readout chain. Bit error rate (BER) measurements have been performed for digital transmission at 40Mb/s and 160Mb/s. BER results for irradiated and un-irradiated PIN receivers confirmed that a considerable operational safety margin still exists following irradiation at the highest anticipated levels.

## I. INTRODUCTION

Data signals will be transmitted from the CMS tracker front-end to the back-end and vice-versa in an analogue or a digital form over numerous optical links. For instance, the  $12 \times 10^6$  microstrip detector channels of the tracker will be connected to the counting room via over 50,000 analogue fibre optic links [1,2]. In contrast, timing, level 1 trigger, monitoring and control signals will be transferred to and from the front-end control module using digital fibre links. Following an R&D program of over several years during which different optical data transmission technologies have been investigated [3], it was concluded that the best combination fulfilling the optical link requirements and development timescales is based on directly modulated edge-emitting laser transmitters, single mode optical fibres, and PIN photodiode receivers [4,5].

(\*) Italtel, Milano

This paper reports on the technical performance of an analogue and a digital one-channel link demonstrator. The link description along with its functionality within the CMS readout system are first briefly reviewed in section 2. Section 3 covers the transmitter, receiver, and the full analogue link characterization whereas the digital link is discussed in section 4.

## II. LINK DESCRIPTION

A simplified representation of the fibre link under evaluation is sketched in Fig. 1. The laser diode converts electrical signals into optical signals, which are then transmitted over a single mode fibre and finally received by a PIN photodiode. For the digital link, the receiver electronic includes a discriminator (not shown in Fig. 1) that produces ECL output logic levels. The optical link concept is discussed in greater details in these proceedings [6].

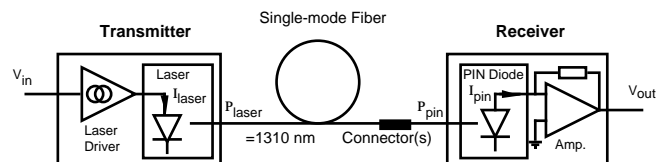


Fig. 1 : Schematic of the optical fibre link with the transmitter (left) and the receiver (right) modules.

One channel analogue and digital link prototypes with the above configuration have been successfully built and tested. The optoelectronic devices are commercially available products\* and are of the same type as the ones intended for the final system. The laser driver and photodiode amplifier are custom developments built from off-the-shelf discrete IC's mounted onto compact printed circuit boards. A driver ASIC has been designed and is being presently evaluated [7].

For easy evaluation of the link in a laboratory environment, a modular test platform is used. It consists of a mother board onto which independent transmitter and receiver daughter boards are plugged in. The

flexible design allows to use these evaluation platforms to test analogue as well as digital links.

In the final system, the input of the transmitter module for the analogue readout of the CMS tracker will be connected to the APV front-end chip. The output of the receiver will be digitized by the ADC on the front-end driver (FED) module. The integration of the link in an emulated readout chain is discussed elsewhere [8]. The digital links will connect the inner detector control ring with the front-end controller (FEC) situated in the counting room [9]. Transmission will occur at 40Mb/s.

All the optoelectronic components situated at the front-end will be exposed to high radiation levels [10]. The effects of gamma and neutron irradiations on laser diodes, PIN diodes, and fibres are the subject of ongoing studies [11,12]. Other technical constraints on the front-end components include low power dissipation, low mass, operation in a magnetic field of up to 4T, and very limited accessibility for maintenance services [13].

### III. ANALOGUE LINK

In the following, the transmitter and receiver are described individually prior to the full link evaluation. A more detailed description of the prototype analogue optical link can be found elsewhere [14].

The specific performance required from the analogue link can be summarized as follows: (a) full scale dynamic range of 7-8bits, with <2% deviation from linearity, (b) overall link noise contribution (rms) equivalent to less than one third of the least significant bit (LSB), and (c) settling time of 15ns to within 1% of the end value.

#### 3.1 ANALOGUE TRANSMITTER

The analogue transmitter is illustrated in Fig. 2.

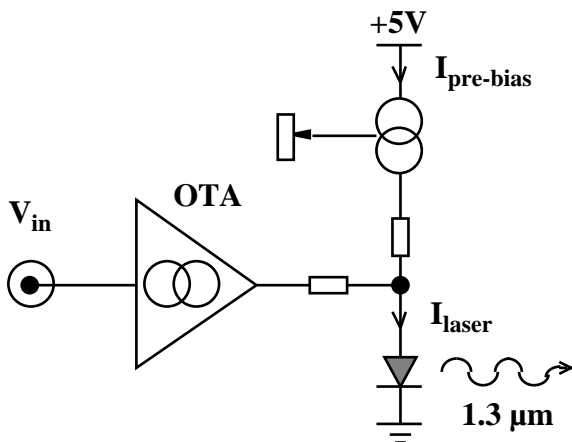


Fig. 2 : Analogue transmitter with the transconductance amplifier (OTA) and the pre-biasing circuitry.

It includes a semiconductor laser and a laser driver. The laser structure is of the double-channel planar buried heterostructure (DCPBH) type with an InGaAsP strained multiple quantum well active region grown on top of an InP substrate [15]. The laser emission wavelength occurs at 1.31 $\mu$ m from band to band transitions in the strained quantum wells. The investigated lasers have a typical threshold current close to 8mA and a slope efficiency 0.22 W/A. The laser die and fibre are actively aligned to each other and mounted onto a common Si-submount with footprint dimensions 2x1.5mm. The resulting compact and low mass sub-assembly is further hermetically encapsulated into a mini-DIL (dual-in-line) ceramic package.

The laser driver provides the dc pre-bias current,  $I_{pre-bias}$ , as well as the modulation current proportional to the input voltage signal  $V_{in}$ . The pre-bias working point is set by adjusting the reference input resistor of a monolithic dual transistor current mirror. The modulation current is controlled by a wide bandwidth (370MHz) operational transconductance amplifier (OTA). The static characteristic and the relative deviation from linearity (RDL) of the laser driver are shown in Fig. 3 for a dc pre-bias current of 11 mA.

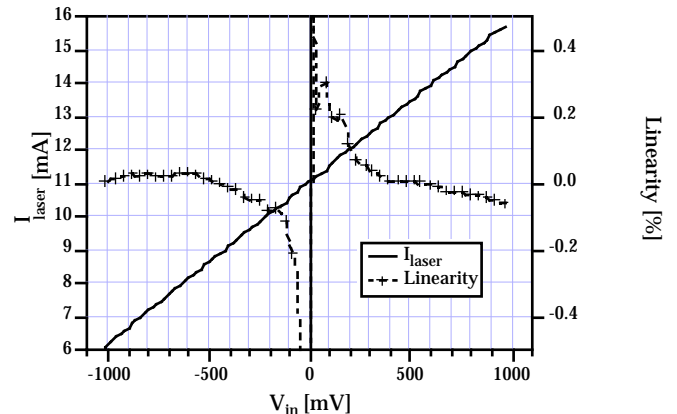


Fig 3 : Static characteristic (left) and relative deviation from linearity of the laser driver for a dc pre-bias current of 11mA.

The laser current,  $I_{laser}$ , corresponds to the sum of the constant dc pre-bias current and the adjustable modulation current. The measured transconductance,  $G_m$ , is 5.2mA/V and is independent of the pre-bias point. Hence, multiplying  $G_m$  by the laser slope efficiency, the transmitter gain is calculated to be 1.14 $\mu$ W/mV. The RDL is defined as the relative distortion with respect to a best linear fit for input signals in the range of  $\pm 900$ mV. The linearity remains well below one percent with diverging values for  $V_{in}$  close to 0 mV since at the origin the RDL becomes undefined.

### 3.2 ANALOGUE RECEIVER

A schematic of the analogue receiver module is shown in Fig. 4.

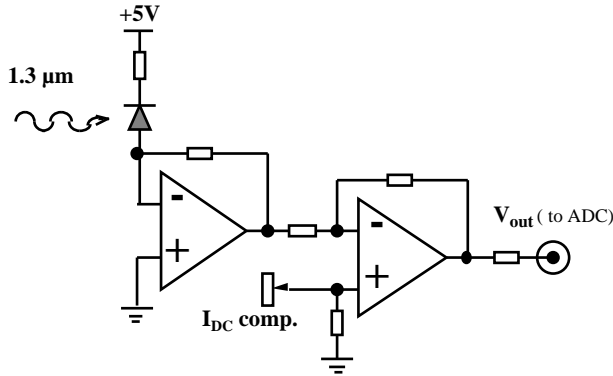


Fig. 4 : Analogue receiver showing the reverse biased PIN photodiode, the transimpedance amplifier, and the post-amplifier with adjustable bias.

It includes the PIN photodiode and the amplifier. The PIN photodiodes consist of a lattice matched InGaAs alloy active layer grown on top of an InP substrate. A heavily doped p-type implant defines the active diameter of 75μm. The tested photodiodes have a typical responsivity  $R_{pin}$  0.96A/W (at 1.31μm). The PIN photodiodes are back illuminated with the InP substrate acting as a transparent optical window at 1.31μm. The fibre light is coupled to the photodiode chip through the use of a micromachined Si-submount onto which both the fibre and the photodiode are attached. The packaging scheme is similar to the laser module with a small footprint Si-submount housed in a mini-DIL package.

The photocurrent of the reverse biased PIN photodiode is converted to a voltage using a transimpedance amplifier. In the final readout system, the voltage output of the amplifier will be connected to the input of the ADC on the FED board. The photodiode is dc-coupled to the amplifier thus allowing the on-line monitoring of the quasi-static link performance. A simple resistive compensation network adapts the receiver operating range to the transmitter dc pre-bias point. The static response of the amplifier is illustrated in Fig. 5 for an offset bias of 0V. The measured transresistance gain,  $R_{Rx}$  9.93k, translates to a receiver gain of 9.53mV/μW if multiplied by the photodiode responsivity ( $R_{pin}=0.96A/W$ ). The amplifier saturates at ±3.2V for an input current range of ±350μA. The RDL is plotted on the right axis of Fig. 5. It is less than 0.2% for a photocurrent range of ±300μA.

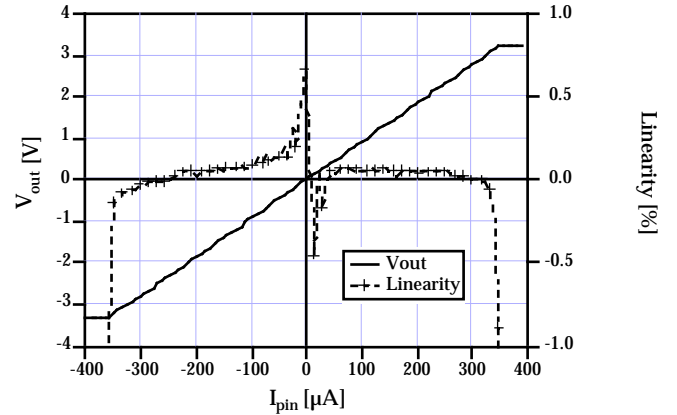


Fig. 5 : Photodiode amplifier static characteristic. The relative deviation from linearity is plotted against the right axis.

### 3.3 FULL ANALOGUE LINK CHARACTERISTIC

#### a) Static characteristic

The link gain is expressed as follows:

$$\frac{V_{out}}{V_{in}} = R_{Rx} \times R_{pin} \times \eta \times G_m \times IL_{connector} \quad (1)$$

where  $R_{Rx}$  is the receiver transresistance gain,  $R_{pin}$  the photodiode responsivity,  $\eta$  the laser slope efficiency,  $G_m$  the laser driver transconductance, and  $IL_{connector}$  the connector insertion losses. The transmitter and receiver fibre pigtailed were linked using a FC-PC optical connector with an average insertion loss,  $IL_{connector}$  of

0.2dB. The static response of the full link is shown in Fig. 6 over the 0 to 3V operating range of the ADC (on the FED).

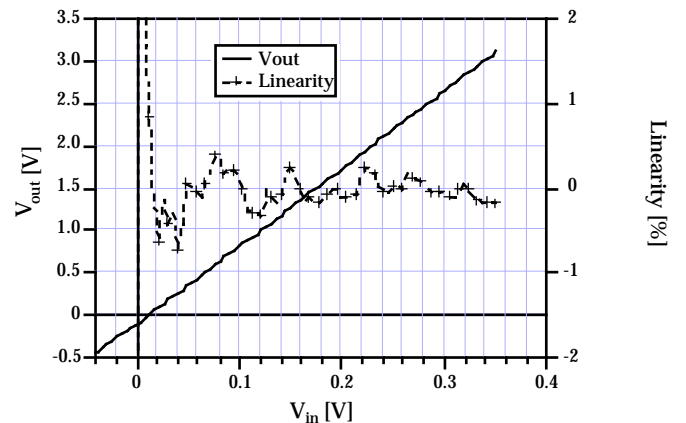


Fig. 6 : Full link transfer characteristic and relative deviation from linearity over the 0-3V operating range of the ADC.

The measured average link gain is 10.5, in close agreement with the 10.3 gain value computed from the independent link component characteristics (Eq. 1). It is worth noting that uncertainty arises from  $\Gamma_{\text{connector}}$  since the insertion losses depend on the mating and/or remating reproducibility.

The relative deviation from linearity (RDL) is plotted against the right axis of Fig. 6. It is calculated from the relative error with respect to a linear fit for input signals between 0 and 300mV, in the same way as was previously done for the laser driver and photodiode amplifier. The full link relative distortion with the current optoelectronic components is well within the 2% linearity specification.

### b) Dynamic characteristic

The link demonstrator step response is shown in Fig. 7. The straight line is the input signal with the scale on the left axis. The dashed line represents the output signal and is plotted against the right axis. The input pulse is typical of a large signal delivered by the front-end APV chip with a rise time of 5ns and a plateau of 20ns. We measure on the output pulse an overshoot of 4% of the pulse height and a settling time of 10ns to within 1% of the end value. It is worth recalling that signals will have to be digitized within the 25ns sample period.

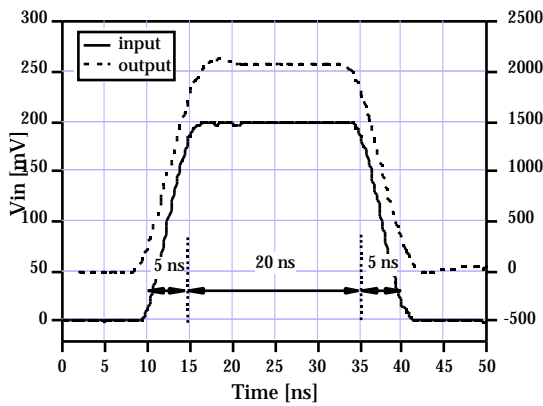


Fig. 7 : Full link step response to an APV representative signal.

The full link frequency response characteristic, shown in Fig. 8, was measured using a spectrum analyzer equipped with a tracking generator. Dots are experimental data and the solid line is a fit using a second order filter. The stimulus input signal was sinusoidal with amplitude  $V(\text{rms})$  75mV and frequencies between 1MHz and 250MHz. The static link gain is 15.1dB (into 50  $\Omega$ ) and is consistent with the dc gain value mentioned above (into high impedance). The -3dB cut-off frequency is 110MHz, essentially

limited by the receiver bandwidth. By applying an inverse Fourier transformation on the fit, the temporal step response was synthesized and the measured 10ns settling time value within 1% was confirmed.

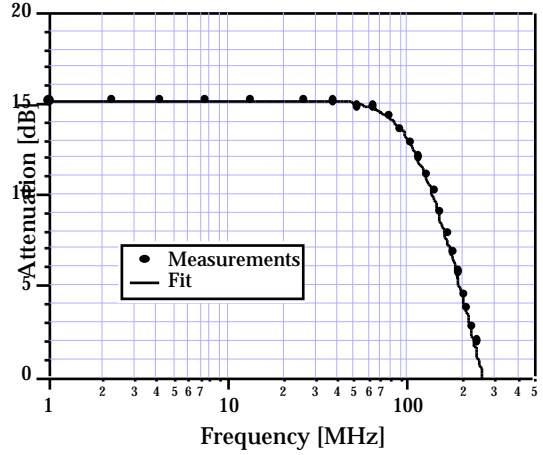


Fig. 8 : Full link frequency response. Dots are the experimental data and the line is a fit using a second order filter.

### c) Noise

Noise measurements are reported in Fig. 9 with the equivalent input noise spectral density and integrated rms noise on the left and right axis, respectively. The equivalent input rms noise (in the full link frequency bandwidth) is 0.7mV, corresponding to a peak SNR 420/1. It can be seen in Fig. 9 that the noise spectral density is not flat over the 110MHz link bandwidth, with a small decline already starting at 10MHz. Work is in progress to determine and locate the major noise sources.

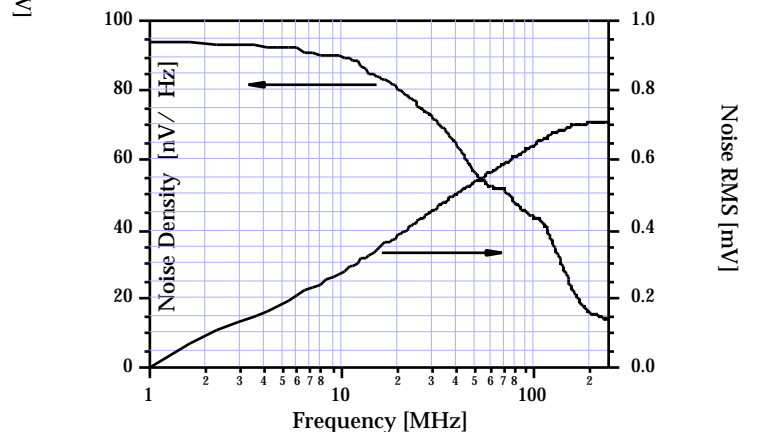


Fig. 9 : Full link equivalent input noise figure.

## IV. DIGITAL LINK

As previously stated, the same optoelectronic components are used in the digital and the analogue link

[6]. The digital links for the control system of the CMS tracker will operate at 40Mb/s and the envisaged number of required links is of the order of few thousands. Besides transmitters, fibres, and connectors, receivers including PIN photodiodes, transimpedance amplifiers, and discriminators will be located in the highly irradiated region of the detector and must therefore be qualified for radiation hardness [13].

A good Figure of Merit of a digital communication system is its bit error rate. The BER is defined as the ratio of wrongly detected bits to the number of transmitted bits. Error bits occur mostly because of noise disturbance at the receiver. If noise sources (thermal noise and shot noise) are described by Gaussian statistics, the BER can be expressed as follows [16]:

$$\text{BER} = \frac{1}{2} \operatorname{erfc} \frac{\text{SNR}}{\sqrt{2}} = \frac{\exp(-\text{SNR}^2/2)}{\text{SNR} \times \sqrt{2}} \quad (2)$$

where the exponential approximation is obtained using asymptotic expansion of the error function. SNR is defined as the peak signal to rms noise power ratio and is assumed to be proportional to the optical power at the receiver,  $P_{\text{pin}}$ .

The BER measurements were performed by inserting an adjustable optical attenuator between the transmitter and the receiver module (see Fig. 1). A pseudo-random NRZ coded bit stream ( $2^{11}-1$ ) was fed into the link and compared to the output data sequence after clock synchronization. The injected optical power,  $P_{\text{laser}}$ , was -3.25dBm and  $P_{\text{pin}}$  was simply obtained by subtracting the attenuation from  $P_{\text{laser}}$  ( $P_{\text{pin}} = P_{\text{laser}} - \text{Att}[\text{dB}]$ ).

Fig. 10 shows oscilloscope eye diagrams at a bit rate of 40Mb/s for received powers of -32.2dBm and -33.7dBm, respectively (these two data points are indicated by tags on the BER plots of Fig. 11). Eye diagrams were obtained by placing the scope in infinite persistence mode and triggering it externally with the clock signal. The data bits were digitized on the falling edges of the clock (also shown in Fig. 10). For an optimized BER, those edges must be at the center of the eye where a clean 1 or 0 may still be found even after pulse width distortion. At -32.2dBm, the BER is  $10^{-12}$  and the eye is wide open with negligible jitter. At -33.7dBm, the BER has increased to  $10^{-7}$  and some multiple crossings and jitter are observed although the eye is far from being completely closed.

The BER plots are shown in Fig 11. The empty and filled symbols correspond to BER at 40Mb/s and 160Mb/s, respectively, with squares representing data taken with un-irradiated photodiodes. The empty circles are BER for PIN diodes having been exposed to a neutron fluence of  $6 \times 10^{14} \text{ n/cm}^2$  and a dose of 100KGy

(LHC-like radiation environment). The dotted lines are fits to Eq. 2, showing excellent agreement with a Gaussian noise probability density function.

The data were corrected for 95% confidence levels (CL) assuming that the occurrence of errors follows a Poisson distribution [17]. For information, reaching a BER of  $10^{-12}$  at 40Mb/s with 95% CL implies testing an error-free link for a minimum of 21 hours. However, fitting experimental data points with Eq. 2 allows to extrapolate to very low BER as long as the receiver noise floor limit is not reached. We can see that BER less than  $10^{-12}$  are easily attained with the present digital link configuration. Irradiating the PIN diodes shifts the received signal level by 5dB but still preserves an excellent safety margin for LHC operation. This 5dB penalty is well correlated with the observed 70% loss in the damaged photodiode responsivity (w.r.t. its pre-irradiated responsivity value) [12].

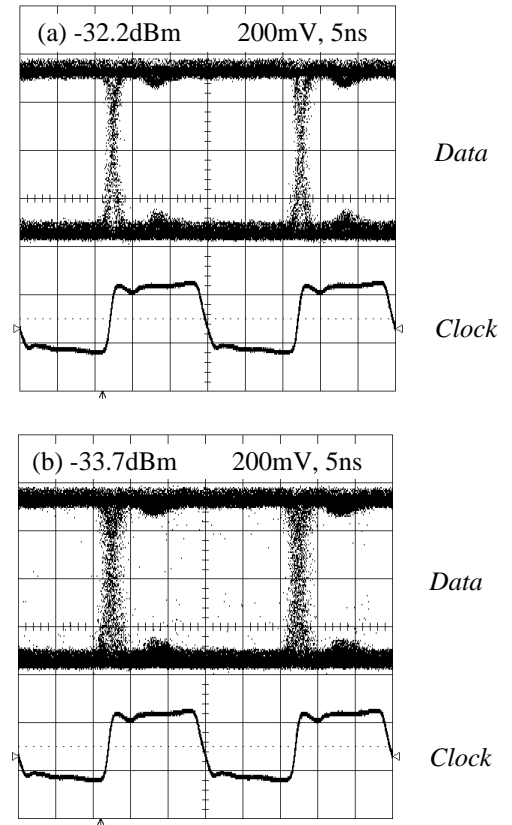


Fig. 10 : Eye diagrams at 40Mb/s with received power at the receiver of (a) -32.2dBm and (b) -33.7dBm. The data bits are strobed on the falling edges of the clock.

The higher BER at 160Mb/s is attributed in part to the clock not being well centered within the eye. Work is in progress to characterize digital links up to 1Gb/s.

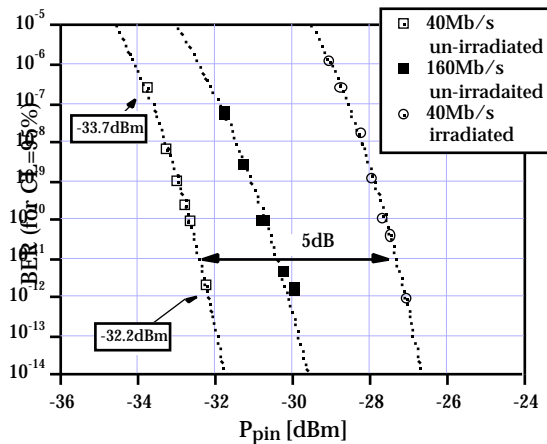


Fig. 11 : BER plot at 40Mb/s and 160Mb/s for irradiated and un-irradiated PIN photodiodes.

## V. CONCLUSION

Analogue and digital prototype link demonstrators based on commercially available optoelectronic devices have been built and fully characterized. Directly modulated 1310nm semiconductor lasers are driven by transconductance amplifiers. The laser light is transmitted over single-mode optical fibres to the receiver circuit boards where it is detected by reverse biased PIN photodiodes coupled to transimpedance amplifiers (and discriminators for digital transmission). The prototype driver and receiver amplifiers are built using discrete commercial IC's. The lasers and PIN assemblies and packages are identical to the ones tested for radiation hardness. The development of 4-way links with laser driver ASIC's is under way.

The static and dynamic performances of the analogue link meet all the requirements for the electronic readout of the tracker with deviation from linearity < 2% and settling time < 10ns to within 1% of the end value. The input equivalent rms noise using currently available lasers is of the order of 0.7mV. With a full link cut-off frequency at 110MHz, a SNR 420/1 has been measured. Regarding the digital link at 40Mb/s, a BER not exceeding  $10^{-12}$  has been demonstrated for a received optical power of -32.2dBm (almost three orders of magnitude less than the injected laser power !). A 5db penalty is reported for irradiated photodiodes still leaving a comfortable safety margin for a reliable operation of the control electronics for the CMS inner tracker.

## ACKNOWLEDGEMENTS

The authors would like to acknowledge Paolo Moreira for fruitful discussions. We also would like to thank Bernard Cornet for assistance in preparing the transmitter and receiver boards as well as F. Pollin and

W. Debeats for their collaboration in the characterization of the digital link.

## REFERENCES

- [1] G. Hall and G. Stefanini, "CMS tracker readout system", CMS TN/94-137
- [2] G. Hall, "Analogue optical data transfer for the CMS tracker", Nucl. Inst. and Meth. A386, 138 (1997)
- [3] RD23 status reports, CERN/DRDC 93-35 (1993), CERN/DRDC 94-38 (1994), CERN/DRDC 95-61 (1995), CERN/LHCC 97-30 (1997)
- [4] G. Hall, G. Stefanini, and F. Vasey, "Fibre optic link technology for the CMS tracker", CMS note 1996/012
- [5] F. Vasey, G. Stefanini, and G. Hall, "Laser based optical links for the CMS tracker: options and choices", CMS note 1997/053
- [6] F. Vasey et al., "Development of rad-hard laser-based optical links for CMS front-ends", these proceedings
- [7] P. Moreira et al., "An integrated laser driver array for analogue data transmission in the LHC experiments", these proceedings
- [8] G. Cervelli et al., "Simulation and characterization of the CMS tracker optical readout chain", these proceedings
- [9] A. Marchioro et al., "A system for timing distribution and control of front-end electronics for the CMS tracker", these proceedings
- [10] M. Huhtinen, "Studies of neutron moderator configurations around the CMS inner tracker and ECAL", CMS TN/96-057
- [11] K. Gill et al., "Effect of neutron irradiation of MQW lasers to  $10^{15}$ n/cm<sup>2</sup>", CMS Note 044 (1997)
- [12] K. Gill et al., "Radiation damage studies of optoelectronic components for the CMS tracker optical links", these proceedings
- [13] G. Stefanini, "An overview of requirements for optical links in LHC experiments", Proceedings of the first workshop on electronics for LHC experiments, Lisbon, 157 (1995)
- [14] V. Arbet-Engels et al., "Prototype analogue optical links for the CMS tracker readout system", CMS Note 075 (1997)
- [15] Y. Sakata et al., "Strained MQW-BH-LDs and integrated devices fabricated by selective MOVPE", Tech. Dig. IPRM'96 (1996)
- [16] P. Bylanski and D. G. W. Ingram, Digital Transmission Systems (Peter Peregrinus LTD., Stevenage, 1980)
- [17] Handbook of Applicable Mathematics, Volume VI, Part A (John Wiley & Sons, 1984)